Journal of Catalysis 258 (2008) 121–130

Contents lists available at ScienceDirect

Journal of Catalysis

www.elsevier.com/locate/jcat

Synthesis and structural characterization of a monomeric di-copper-substituted silicotungstate $[\gamma\text{-}H_2SiW_{10}O_{36}Cu_2(\mu\text{-}1,1\text{-}N_3)_2]^{4-}$ and the catalysis of oxidative homocoupling of alkynes

Kazuya Yamaguchi [a,b], Keigo Kamata [a,b], Syuhei Yamaguchi [b], Miyuki Kotani [b], Noritaka Mizuno [a,b,*]

[a] Department of Applied Chemistry, School of Engineering, The University of Tokyo, 7-3-1 Hongo, Bunkyo-ku, Tokyo 113-8656, Japan
[b] Core Research for Evolutional Science and Technology (CREST), Japan Science and Technology Agency (JST), 4-1-8 Honcho, Kawaguchi, Saitama 332-0012, Japan

ARTICLE INFO

Article history:
Received 21 March 2008
Revised 29 May 2008
Accepted 3 June 2008
Available online 1 July 2008

Keywords:
Alkyne
Copper
Diyne
Homocoupling
Polyoxometalate

ABSTRACT

The di-copper-substituted γ-Keggin silicotungstate with bis-μ-1,1-azido ligands $TBA_4[\gamma\text{-}H_2SiW_{10}O_{36}Cu_2(\mu\text{-}1,1\text{-}N_3)_2]$ (**1**, TBA = tetra-*n*-butylammonium) was synthesized in an aqueous medium. The crystal structure of the anion part of **1** was a monomer of the basal–basal end-on diazido-bridged di-copper-substituted γ-Keggin silicotungstate. The NMR and CSI-MS spectra of **1** in organic solvents, such as acetonitrile, benzonitrile, and 1,2-dichloroethane, showed that complex **1** was present as a monomer of the di-copper-substituted γ-Keggin silicotungstate. Complex **1** could act as an effective homogeneous catalyst for the oxidative homocoupling of various types of alkynes, including aromatic, aliphatic, and heteroatom-containing ones. The reaction possibly proceeds as follows: First, the ligand exchange proceeds between the azido groups in **1** and alkynyl groups to form the corresponding diyne with the reduced copper(I) species via the di-copper(II)-alkynyl intermediate, then the reduced species is reoxidized by molecular oxygen, and the oxidized species reacts with an alkyne to regenerate the alkynyl intermediate.

1. Introduction

Polyoxometalates are attractive compounds used in various fields, including analytical chemistry, medicine, electrochemistry, photochemistry, and especially catalysis [1–8]. Recently, interest in the catalysis of transition metal-substituted polyoxometalates, synthesized by the introduction of substituent metal ions into the vacant site(s) of lacunary polyoxometalates, has been growing because of their unique reactivity, which depends on the composition and structure of the active sites [1–8]. Since the synthesis of the di-lacunary $[\gamma\text{-}SiW_{10}O_{36}]^{8-}$ was reported by Tézé and Hervé [9], several di-metal-substituted polyoxometalates with the γ-Keggin framework have been synthesized and applied to the selective "green" oxidation reactions with molecular oxygen or hydrogen peroxide as the sole oxidant [1–8].

The azido ion (N_3^-) is well known to be a versatile ligand that can bridge two or more transition metals [10,11]. Recently, various transition metal-substituted polyoxometalates with azido ligands have been synthesized [12–15]. Mialane et al. reported a mono-μ-1,1-azido-bridged di-nickel-substituted phosphotungstate $KRb_5[(\alpha\text{-}PW_{10}O_{37})(Ni(H_2O))_2(\mu\text{-}1,1\text{-}N_3)]\cdot 19H_2O$ [12]. Successively, di-copper-substituted silicotungstates, $KNaCs_{10}[\{\gamma\text{-}SiW_{10}O_{36}Cu_2(H_2O)(\mu\text{-}1,1\text{-}N_3)_2\}_2]\cdot 26H_2O$ (**2**) [13] and $TEA_4TBA_2H_2[(\gamma\text{-}SiW_{10}O_{36})_2Cu_4(\mu\text{-}1,1,1\text{-}N_3)_2(\mu\text{-}1,1\text{-}N_3)_2]$ (**3**, TEA = tetraethylammonium) [14], were reported by the same group (Fig. 1). Complexes **2** and **3** have dimeric structures and are composed of two $[SiW_{10}O_{36}Cu_2(N_3)_2]^{6-}$ subunits, with differing connection modes of the ligands [13,14].

Recently, many applications of 1,3-diyne derivatives (both symmetric and nonsymmetric ones) as key structural elements for natural product synthesis, polymer chemistry, supramolecular chemistry, and material science have been reported [16–18]. In addition, electronic and optical properties of extensively π-conjugated systems have spurred research into new linear origoacetylenic compounds in which 1,3-diyne derivatives can be used as precursors [16]. Consequently, much attention has been given to the efficient and selective synthesis of 1,3-diyne derivatives. One of the most widely used synthesis procedures for synthesizing 1,3-diyne derivatives is an oxidative alkyne–alkyne homocoupling reaction. Stoichiometric amounts of copper salts generally have been used under Glaser conditions [19], and, alternatively, catalytic amounts of copper salts with appropriate nitrogen bases (ligands or solvents) and molecular oxygen have been used under Hay [20] or Eglinton conditions [21] for the oxidative alkyne–alkyne homocoupling reactions [22–28]. But the yields of aliphatic 1,3-diynes by

* Corresponding author at: Department of Applied Chemistry, School of Engineering, The University of Tokyo, 7-3-1 Hongo, Bunkyo-ku, Tokyo 113-8656, Japan. Fax: +81 3 5841 7220.
E-mail address: tmizuno@mail.ecc.u-tokyo.ac.jp (N. Mizuno).

0021-9517/$ – see front matter
doi:10.1016/j.jcat.2008.06.004

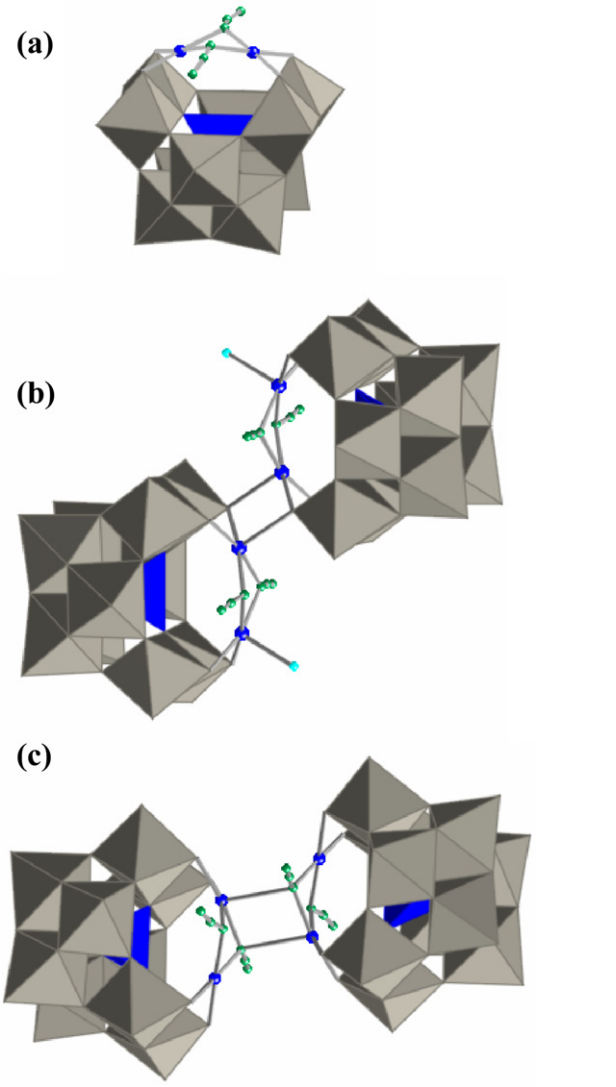

Fig. 1. Polyhedral representations of the anion parts of (a) $TBA_4[\gamma\text{-}H_2SiW_{10}O_{36}Cu_2(\mu\text{-}1,1\text{-}N_3)_2]$ (this study) (**1**) [36], (b) $KNaCs_{10}[\{\gamma\text{-}SiW_{10}O_{36}Cu_2(H_2O)(\mu\text{-}1,1\text{-}N_3)_2\}_2]\cdot 26H_2O$ (**2**) [13], and (c) $TEA_4TBA_2H_2[(\gamma\text{-}SiW_{10}O_{36})_2Cu_4(\mu\text{-}1,1,1\text{-}N_3)_2(\mu\text{-}1,1\text{-}N_3)_2]$ (**3**) [14]. Gray octahedra and blue tetrahedra show the $[WO_6]$ and $[SiO_4]$ units, respectively. Blue, green, and light blue spheres show the copper, nitrogen (azido), oxygen (water) atoms, respectively. (For interpretation of the references to color in this figure legend, the reader is referred to the web version of this article.)

the homocoupling reactions of aliphatic alkynes under the Hay or Eglinton conditions in the presence of copper salts generally have been only low to moderate [19–28]. Although the oxidative homocoupling of aliphatic alkynes with combined catalysts of copper and palladium salts can proceed efficiently, these systems have several disadvantages, including (i) the use of expensive palladium catalysts, (ii) the need for bases and co-catalysts (copper salts), and (iii) difficult catalyst recovery [29–35]. Thus, the development of the widely usable efficient alkyne–alkyne homocoupling systems remains a challenge. The scope and limitations of copper- and/or palladium-mediated homocoupling systems have been reviewed in more detail previously [16].

Recently, we reported that a di-copper-substituted γ-Keggin silicotungstate $TBA_4[\gamma\text{-}H_2SiW_{10}O_{36}Cu_2(\mu\text{-}1,1\text{-}N_3)_2]$ (**1**) acts as an effective homogeneous catalyst for the oxidative alkyne–alkyne homocoupling reactions [Eq. (1)] [36]. In this paper, we report details of the synthesis procedure and structural characterization of the di-copper-substituted γ-Keggin silicotungstate **1** in solid and solution states. Furthermore, the scope of the **1**-catalyzed oxidative alkyne–alkyne homocoupling is extended, and 13 new entries are added [36]. We also discuss the possible reaction mechanism for the present **1**-catalyzed homocoupling in more detail [36].

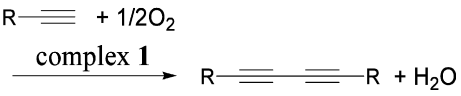

(1)

2. Experimental

2.1. General

IR spectra were measured with a Jasco FT/IR-460 Plus device using KBr disks. NMR spectra were recorded at 298 K on JEOL JNM-EX-270 spectrometer (^{1}H, 270 MHz; ^{13}C, 67.8 MHz; ^{29}Si, 53.45 MHz; ^{183}W, 11.20 MHz). Chemical shifts (δ) were reported in ppm downfield from the internal TMS for ^{1}H and ^{13}C, external TMS (in $CDCl_3$) for ^{29}Si, and external Na_2WO_4 (in D_2O) for ^{183}W. UV–vis spectra were recorded on a Jasco V-570 spectrometer with a Unisoku thermostatic cell holder (USP-203). GC analyses were performed on Shimadzu GC-2014 with a flame ionization detector equipped with a TC-5 capillary column (internal diameter = 0.25 mm, length = 60 m) or a TC-1 capillary column (internal diameter = 0.25 mm, length = 30 m). Mass spectra were recorded on Shimadzu GCMS-QP2010 equipped with a TC-5HT capillary column (internal diameter = 0.25 mm, length = 30 m). CSI-MS spectra were recorded on JEOL JMS-T100LC. Typical measurement conditions were orifice voltage, −95 V; spray temperature, 263 K; and ion source temperature, room temperature. $Na_2WO_4\cdot 2H_2O$, NaN_3, and copper salts were obtained from Wako or Kanto (reagent grade) and used as received. Copper(I) phenylacetylide was obtained from Alfa Aesar (reagent grade) and used as received. Solvents and alkynes were obtained from Tokyo Kasei or Aldrich (reagent grade) and purified before use [37]. The di-copper-substituted silicotungstate **1** was synthesized as described previously [36] (see Supporting information).

2.2. Procedure for oxidative alkyne–alkyne homocoupling

The oxidative alkyne–alkyne homocoupling was carried out as follows. First, **1** (2.2 mol% with respect to alkyne), alkyne (1 mmol), and benzonitrile (1 mL) were successively placed into a glass reactor. The reaction mixture was stirred at 373 K under 1 atm of molecular oxygen. The yield was periodically determined by GC analysis. After the reaction was completed, 20 mL of diethylether was added to the solution. The precipitated catalyst was recovered by filtration (95% recovery), washed with diethylether (ca. 50 mL), and dried in vacuo before being recycled. Isolation and purification of diynes were carried out by column chromatography on silica gel, using *n*-hexane as an eluent. All products were confirmed by comparing their GC retention times, mass, and NMR spectra with those of authentic samples. The purity of isolated products was determined by ^{1}H NMR and was >95% in all cases.

3. Results and discussion

3.1. Synthesis and characterization of $TBA_4[\gamma\text{-}H_2SiW_{10}O_{36}Cu_2(\mu\text{-}1,1\text{-}N_3)_2]$ (**1**)

The TBA salt of a di-copper-substituted silicotungstate with bis-μ-1,1-azido ligands (**1**) was obtained by the reaction of $K_8[\gamma\text{-}SiW_{10}O_{36}]$ with two equivalents of $CuCl_2$ and an excess amount of NaN_3 in aqueous solution at room temperature, followed by the addition of TBABr. The detailed procedure is as follows. First, $CuCl_2$ (0.090 g, 0.67 mmol, two equivalents with respect to $[\gamma\text{-}SiW_{10}O_{36}]^{8-}$) in water (20 mL) was added to a suspension of

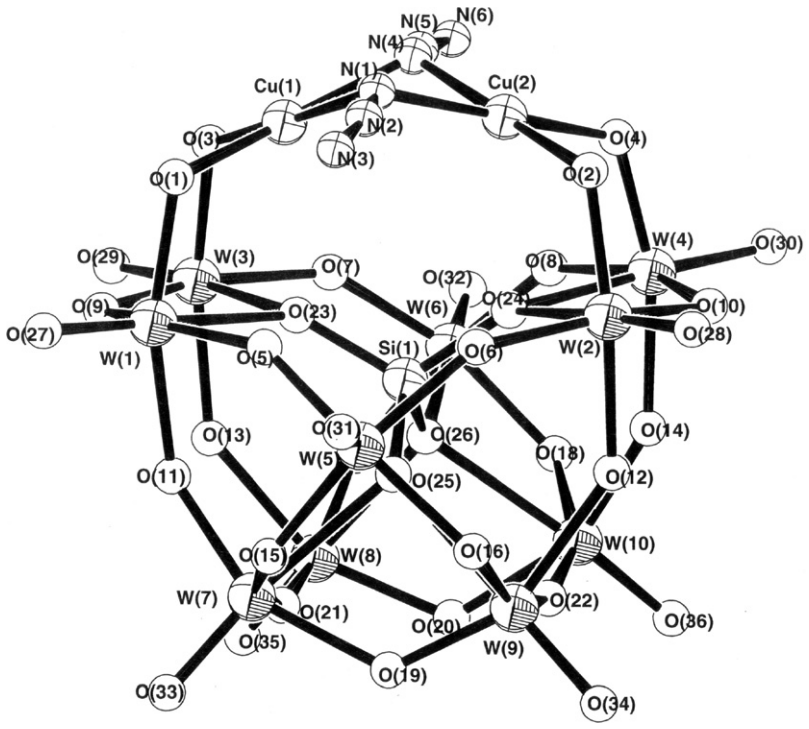

Fig. 2. ORTEP drawing of the anion part of **1** drawn at 30% probability level.

$K_8[\gamma\text{-}SiW_{10}O_{36}]\cdot 12H_2O$ (1.00 g, 0.335 mmol) in water (20 mL). After 1 min, NaN_3 (0.114 g, 1.75 mmol, 5.2 equivalents with respect to $[\gamma\text{-}SiW_{10}O_{36}]^{8-}$) in water (20 mL) was added, followed by the immediate addition of TBABr (2.00 g, 6.20 mmol) in water (20 mL). The pH of the mixture was adjusted to 6.0 with 1.0 M aqueous HNO_3 solution, followed by stirring for 20 min at room temperature. The green precipitate of **1** was collected by filtration and washed with an excess amount of water (0.78 g, 64% yield based on $K_8[\gamma\text{-}SiW_{10}O_{36}]\cdot 12H_2O$).

The elemental analysis of **1** demonstrated a Si:Cu:W ratio of 1:2:10. The IR spectrum of **1** showed bands of the asymmetric and symmetric stretching vibrations of the μ-1,1-azido ligands at 2078 and 1274 cm^{-1}, respectively [38]. Complex **1** was found to be soluble in various organic solvents, including acetonitrile, benzonitrile, dichloromethane, 1,2-dichloroethane, DMF, and DMSO, and the single crystal suitable for X-ray analysis was successfully obtained by recrystallization in a mixed solvent of 1,2-dichloroethane and dichloromethane with vapor diffusion of diethylether. The molecular structure of **1** is illustrated in Fig. 2. As shown, the anion part of **1** is a monomer of the basal–basal end on diazido-bridged di-copper-substituted γ-Keggin silicotungstate. The selected bond lengths and angles are summarized in Table 1. The Cu(1)···Cu(2) distance, $d_{Cu(1)\cdots Cu(2)}$, was 2.812(5) Å, shorter than those of dimeric complexes **2** [$d_{Cu(1)\cdots Cu(2)} = 2.979(1)$ Å] [13] and **3** [2.875(3) Å] [14]. The average Cu–N–Cu angle, θ_{av}, was 91.5°, smaller than those of **2** (96.7°) [13] and **3** (94.6°) [14].

Recently, two di-copper-substituted silicotungstate *dimers* **2** [13] and **3** [14] were reported by Mialane et al. (Figs. 1b and 1c). Complex **2** was synthesized in aqueous media with hydrophilic alkali metals (K, Na, and Cs) as counter cations [13]. Complex **3** was synthesized in organic solvents (an acetonitrile–methanol mixture) with lyophilic alkylammoniums (TEA and TBA) as mixed counter cations [14]. Whereas the connection modes of the ligands differed, both conditions gave the dimer of the $[SiW_{10}O_{36}Cu_2(N_3)_2]^{6-}$ subunit in the solid states. In sharp contrast, the synthesis in aqueous media with lyophobic TBA as a counter cation afforded the monomer form of the basal–basal end on diazido-bridged di-copper-substituted γ-Keggin silicotungstate under the present conditions.

Table 1
Selected structural parameters for **1**

	Length (Å)		Length (Å)
Cu(1)–O(1)	1.89(2)	Cu(1)–O(3)	1.95(2)
Cu(1)–N(1)	1.94(3)	Cu(1)–N(4)	1.99(3)
Cu(2)–O(2)	1.93(2)	Cu(2)–O(4)	1.93(2)
Cu(2)–N(1)	1.93(3)	Cu(2)–N(4)	1.96(3)
Cu(1)···Cu(2)	2.812(5)		
W=O_{av}	1.68	W–$O_{Cu\ av}$	1.85
W–$O_{Si\ av}$	2.31	W–$O_{W\ av}$	1.92
Si–O_{av}	1.63		
	Angle (deg.)		Angle (deg.)
Cu(1)–N(1)–Cu(2)	93(1)	Cu(1)–N(4)–Cu(2)	90(1)
O(1)–Cu(1)–O(3)	93.9(9)	O(1)–Cu(1)–N(1)	92(1)
O(1)–Cu(1)–N(4)	170(1)	O(3)–Cu(1)–N(1)	173(2)
O(3)–Cu(1)–N(4)	95(1)	N(1)–Cu(1)–N(4)	77(1)
O(2)–Cu(2)–O(4)	92.4(9)	O(2)–Cu(2)–N(1)	96(1)
O(2)–Cu(2)–N(4)	170(1)	O(4)–Cu(2)–N(1)	170(1)
O(4)–Cu(2)–N(4)	91(1)	N(1)–Cu(2)–N(4)	78(1)

The existence of four TBA cations per the anion part of **1** implies a −4 charge of the cluster anion. The bond valence sum (BVS) [39,40] values of copper (1.84–1.87), tungsten (5.88–6.53), and silicon (3.91) indicate that the respective valences in **1** were +2, +6, and +4. Thus, based on the charge balance, two protons were associated with the cluster anion. The BVS values of 1.24 for O(12) and 1.35 for O(13) were lower than those for the other oxygen atoms in **1** (1.54–2.27), suggesting that O(12) and O(13) were monoprotonated. These results and elemental analysis show that the formula of **1** was $TBA_4[\gamma\text{-}H_2SiW_{10}O_{36}Cu_2(\mu\text{-}1,1\text{-}N_3)_2]$. The formation of **1** anion is expressed by the following equation:

$$[\gamma\text{-}SiW_{10}O_{36}]^{8-} + 2Cu^{2+} + 2N_3^- + 2H^+ \rightarrow [\gamma\text{-}H_2SiW_{10}O_{36}Cu_2(\mu\text{-}1,1\text{-}N_3)_2]^{4-} \quad (2)$$

To investigate the state of complex **1** in solution, NMR spectra were measured in organic solvents. The ^{29}Si NMR spectrum

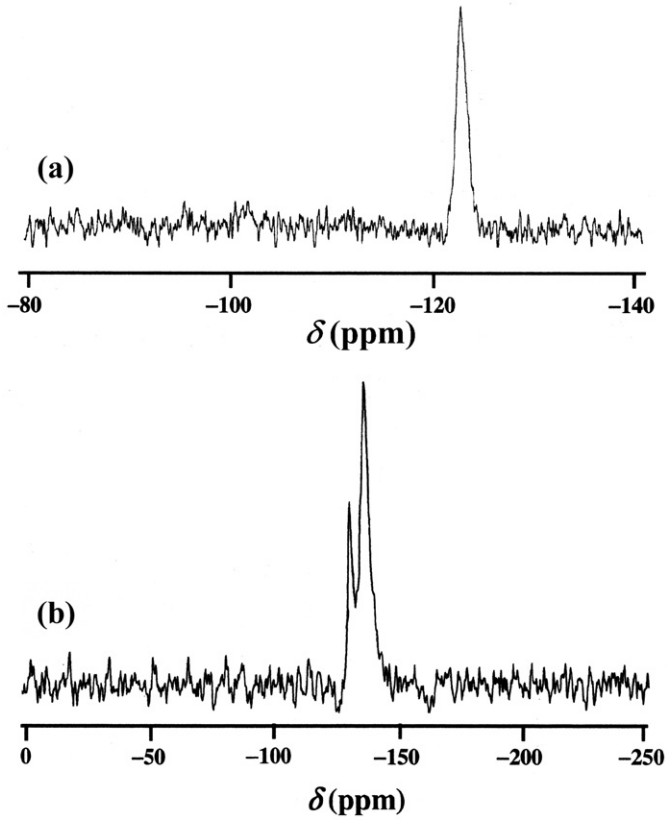

Fig. 3. (a) ^{29}Si and (b) ^{183}W NMR spectra of **1** in CD_3CN.

of the acetonitrile (CD_3CN) solution of **1** gave a chemical shift at −122.8 ppm, suggesting that compound **1** is a single species in acetonitrile (Fig. 3a). The ^{29}Si NMR resonance was shifted to upfield ($\Delta\delta = 39.4$ ppm) to that of $[\gamma\text{-}SiW_{10}O_{36}]^{8-}$, and the line was broadened. This upfield shift and line broadening are likely due to the effect of the paramagnetic d^9 copper(II) species. The ^{183}W NMR spectrum exhibited two signals at −130.6 and −136.3 ppm, with a respective intensity ratio of 1:2 (Fig. 3b). The signals of four tungsten atoms, W(1), W(2), W(3), and W(4), bound to the copper units were not observed; a similar disappearance of ^{183}W NMR signals has been reported for a copper(II)-substituted polyoxometalate $[\alpha_2\text{-}P_2W_{17}O_{61}Cu(II)Br]^{9-}$ [41]. This is likely due to the paramagnetic coupling with d^9 copper(II) species [41]. The structural symmetry of tungsten atoms (C_{2v}) suggests that the cluster framework of **1** maintained the γ-Keggin structure in acetonitrile.

Next, the cold-spray ionization mass (CSI-MS) spectra of **1** were measured in organic solvents. It has been reported that the alkali metal salts of polyoxometalates are soluble only in water and give very complex MS spectra due to the side reactions [42]. In contrast, the TBA salts of polyoxometalates in organic solvents give well-defined MS spectra, related to the accessible protonation sites of the clusters in solution [42]. The CSI-MS spectrum of the acetonitrile solution of **1** exhibited mainly a +1-charged ion peak at $m/z = 3866$, which can be assigned to $\{TBA_5[H_2SiW_{10}O_{36}Cu_2(N_3)_2]\}^+$ (Fig. 4). Ion peaks corresponding to dimer species and non-copper-substituted silicotungstates were hardly observed in the CSI-MS spectrum. The CSI-MS spectrum of **1** in benzonitrile and 1,2-dichloroethane also exhibited similar ion peaks that can be assigned to the monomer species. All of these NMR and CSI-MS data suggest that complex **1** was present as a monomer of the di-copper-substituted γ-Keggin silicotungstate in these solutions.

3.2. Scope of the *1*-catalyzed oxidative alkyne–alkyne homocoupling

The **1**-catalyzed oxidative homocoupling of ethynylbenzene (**4a**) to 1,4-diphenyl-1,3-butadiyne (**5a**) was carried out in various sol-

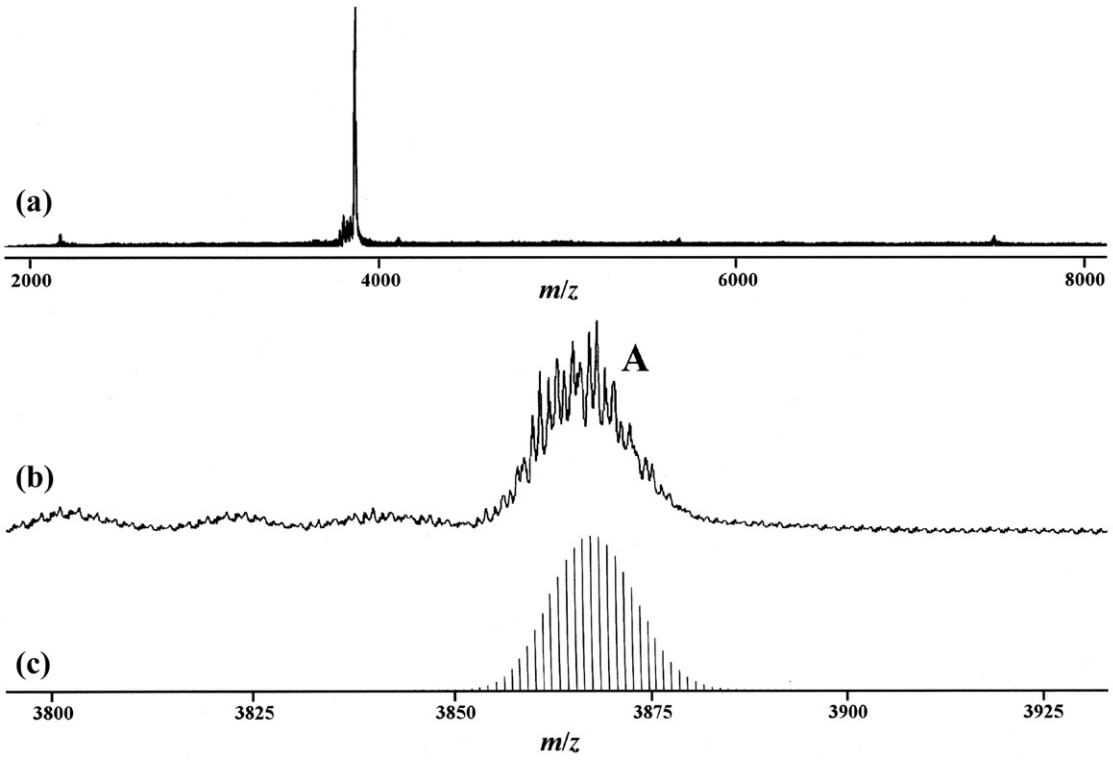

Fig. 4. CSI-MS spectra of **1**; (a) $m/z = 2000$–8000 and (b) $m/z = 3800$–3925; $m/z = 3866$ $\{TBA_5[H_2SiW_{10}O_{36}Cu_2(N_3)_2]\}^+$ (**A**). The lines in (c) are the calculated pattern of $\{TBA_5[H_2SiW_{10}O_{36}Cu_2(N_3)_2]\}^+$.

Table 2
Effect of solvents on the **1**-catalyzed oxidative homocoupling of **4a**[a]

Entry	Solvent[b]	Additive	Time (h)	Yield of **5a**[c] (%)
1	Benzonitrile	–	3	91
2[d]	Benzonitrile	–	6	86
3	DMF	–	3	39
4	DMF	–	24	63
5	DMF	Benzonitrile (0.5 mmol)	24	88
6	DMF	Water (1 mmol)	3	9
7	DMF	MS4A (200 mg)	3	90
8	DMSO	–	3	39
9	DMSO	MS4A (200 mg)	3	86
10	Acetonitrile	–	3	15
11	1,2-Dichloroethane	–	3	4
12	Nitrobenzene	–	3	3
13	Toluene	–	3	2
14	Acetic acid	–	3	2

[a] Reaction conditions: **1** (2.2 mol% with respect to **4a**), **4a** (1 mmol), solvent (1 mL), 373 K, O_2 (1 atm).
[b] DMF = *N*,*N*-dimethylformamide. DMSO = dimethyl sulfoxide. MS4A = Molecular Sieve 4A (pretreated at 423 K).
[c] Determined by GC analysis using naphthalene as an internal standard.
[d] The reaction was carried out in air (1 atm).

Table 3
Oxidative homocoupling of **4a** by various catalysts[a]

Entry	Catalyst	Yield of **5a**[b] (%)
1	**1**	91
2	$TBA_4[\alpha\text{-}H_2SiW_{11}CuO_{39}]$	2
3[c]	$TBA_4[\gamma\text{-}SiW_{10}O_{34}(H_2O)_2]$	<1
4[d]	$TBA_4[\gamma\text{-}SiW_{10}O_{34}(H_2O)_2] + CuCl_2$	5
5	$Cu(OAc)_2$	10
6	$CuCl_2$	4
7	CuCl	7
8	CuI	2
9	$[Cu(CH_3CN)_4]PF_6$	<1
10	Cu(I) phenylacetylide	<1
11	none	<1

[a] Reaction conditions: catalyst (Cu: 4.4 mol% with respect to **4a**), **4a** (1 mmol), benzonitrile (1 mL), 373 K, 3 h, O_2 (1 atm).
[b] Determined by GC analysis using naphthalene as an internal standard.
[c] 2.2 mol%.
[d] Mixture of $TBA_4[\gamma\text{-}SiW_{10}O_{34}(H_2O)_2]$ (2.2 mol%) and $CuCl_2$ (4.4 mol%) was used.

vents (Table 2). Among the solvents tested (with no additives), benzonitrile gave the corresponding diyne **5a** in the highest yield, 91% (entry 1). In benzonitrile, the reaction proceeded efficiently even in air (1 atm) (entry 2). Polar aprotic solvents, such as DMF, DMSO, and acetonitrile, gave **5a** in moderate yields (entries 3, 8, and 10), whereas nonpolar and protic polar solvents, such as 1,2-dichloroethane, toluene, and acetic acid, gave low yields of **5a** (entries 11–14). In the **1**-catalyzed homocoupling of **4a** in benzonitrile, an equimolar amount of benzamide (formed through the hydration of benzonitrile) with respect to the corresponding diyne **5a** was formed as a co-product. A separate experiment confirmed that the homocoupling reaction was strongly inhibited by the presence of water (entry 6 vs entry 3). These findings suggest that benzonitrile likely acted as a scavenger to remove the water formed by the homocoupling reaction. The amount of benzonitrile can be reduced. When the oxidative homocoupling of **4a** in DMF was carried out in the presence of stoichiometric amounts of benzonitrile with respect to the amount of water formed, an 88% yield of **5a** was obtained over 24 h (entry 5) (cf. 63% yield without benzonitrile; entry 4). In addition, the reaction of **4a** in DMF and DMSO with Molecular Sieve 4A (200 mg, pretreated at 423 K) gave **5a** in 90% and 86% yields, respectively, over 3 h (entries 7 and 9). The foregoing results demonstrate that benzonitrile is not a special solvent,

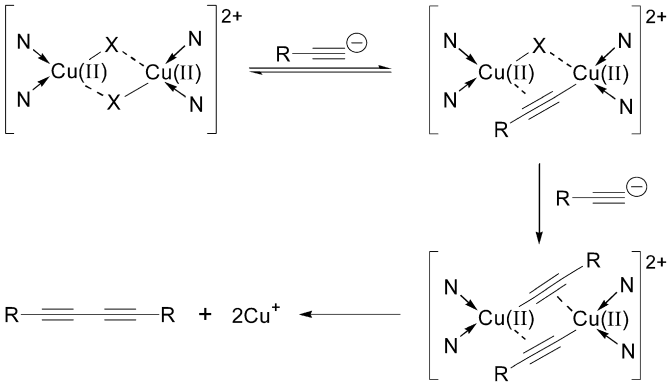

Scheme 1. Possible reaction mechanism for the copper-mediated alkyne–alkyne homocoupling proposed by Bohlmann and co-workers [43]. This mechanism has been well accepted [16]. (N = nitrogen bases, X = Cl^-, OAc^-, etc.)

and that various kinds of solvents can be used for the present homocoupling reaction in the presence of water scavengers.

The effect of the catalysts was investigated (Table 3). In the absence of catalysts or in the presence of simple copper(I) and copper(II) salts, the reaction hardly proceeded under the present conditions (entries 5–11). The mono-copper-substituted silicotungstate $TBA_4[\alpha\text{-}H_2SiW_{11}CuO_{39}]$ (entry 2), the non-copper-substituted silicotungstate $TBA_4[\gamma\text{-}SiW_{10}O_{34}(H_2O)_2]$ (entry 3), and a mixture of $TBA_4[\gamma\text{-}SiW_{10}O_{34}(H_2O)_2]$ and $CuCl_2$ (entry 4) were almost inactive. This demonstrates that the di-copper core $\{Cu_2(\mu\text{-}1,1\text{-}N_3)_2\}$ in **1** played an important role in the present oxidative alkyne–alkyne homocoupling. Bohlmann et al. [43] proposed that the copper(II)-catalyzed alkyne–alkyne homocoupling reaction proceeds via the formation of the di-copper(II)–alkynyl intermediate $\{Cu(II)_2(\mu\text{-}C{\equiv}CR)_2\}$, which would collapse directly to the 1,3-diyne products, as shown in Scheme 1. This reaction mechanism generally has been accepted [16]. The present homocoupling likely proceeded via the formation of similar alkynyl species (see Section 3.3).

In the present study, we also investigated the scope of the **1**-catalyzed oxidative homocoupling reaction. We recently reported on the **1**-catalyzed oxidative alkyne–alkyne homocoupling [36]. In the present work, we extended the scope of the investigation and included 13 new entries, as shown in Table 4. The catalytic oxidative homocoupling reactions of aromatic alkynes (**4a**–**4m**) with electron-donating as well as electron-withdrawing substituents gave the corresponding aromatic diynes in excellent yields (entries 1–18). The positions of the substituents on aromatic rings did not affect the reaction: The reaction rates for the oxidative coupling of 2-, 3-, and 4-methylethynylbenzenes were almost the same (entries 8–10). No dehalogenation occurred in the case of halogen-substituted ethynylbenzenes (**4i**–**4k**) (entries 14–16). The reaction of the nitrogen- (**4l**, **4n**, and **4o**) and sulfur-containing (**4p**) alkynes also proceeded smoothly and gave the corresponding diynes in high yields (entries 17, 19–21). Of note, the less reactive aliphatic terminal alkynes (**4q**–**4v**) [19–28] were efficiently oxidized to give the corresponding aliphatic diynes in high yields (entries 22–27). Propargylic alcohols (**4w**–**4y**) and amine (**4z**) also gave the corresponding diynes (entries 28–31). These findings indicate that the present system has very wide applicability, and that various kinds of structurally diverse alkynes (including aromatic, aliphatic, and heteroatom-containing ones) can be selectively converted to the corresponding diynes in the presence of **1**.

Complex **1** can be applied to larger-scale diyne production. For example, in a 20-mmol scale reaction of **4a** (**1**; 0.2 mol%, PhCN; 20 mL, 373 K, 18 h), the turnover number (TON = amount of **1a** consumed/amount of **1**) reached up to 468, the highest value reported for the copper-mediated oxidative alkyne–alkyne homo-

Table 4
Oxidative alkyne–alkyne homocoupling catalyzed by **1**[a]

Entry	Alkyne	Time (h)	Yield of diyne[b] (%)
1	Ethynylbenzene (**4a**)	3	91 (88)
2[c]	**4a**	3	94
3[c]	**4a**	3	82
4[c]	**4a**	3	88
5[c]	**4a**	3	80
6[c]	**4a**	3	78
7	Ethynylbenzene-d_1 (**4b**)	3	87
8	2-Methylethynylbenzene (**4c**)	3	95
9	3-Methylethynylbenzene (**4d**)	3	97 (93)
10	4-Methylethynylbenzene (**4e**)	3	95 (97)
11	4-*n*-Penthylethynylbenzene (**4f**)	3	96 (64)
12	3-Methoxyethynylbenzene (**4g**)	3	91 (90)
13	4-Methoxyethynylbenzene (**4h**)	3	97 (82)
14	4-Fluoroethynylbenzene (**4i**)	3	96 (89)
15	3-Chloroethynylbenzene (**4j**)	3.5	90 (93)
16	4-Bromoethynylbenzene (**4k**)	4.5	94 (90)
17	3-Aminoethynylbenzene (**4l**)	5	90
18	1-Ethynylnaphthalene (**4m**)	4	93
19	3-Ethynylpyridine (**4n**)	2	95 (82)
20	4-Ethynylpyridine (**4o**)	2	83
21	3-Ethynylthiophene (**4p**)	4	92
22	1-Hexyne (**4q**)	5	91 (80)
23	3,3-Dimethyl-1-butyne (**4r**)	5	90
24	1-Octyne (**4s**)	5	91 (86)
25	1-Decyne (**4t**)	7	92 (89)
26	1-Hexadecyne (**4u**)	8	76
27	6-Chloro-1-hexyne (**4v**)	7	76
28	2-Propyn-1-ol (**4w**)	18	85
29	2-Methyl-3-butyn-2-ol (**4x**)	2	>99 (99)
30	1-Ethynylcyclohexanol (**4y**)	4	90 (82)
31	*N*,*N*-Dimethyl-2-propyn-1-amine (**4z**)	4	91

[a] Reaction conditions: **1** (2.2 mol% with respect to alkyne), alkyne (1 mmol), benzonitrile (1 mL), 373 K, O_2 (1 atm).
[b] Determined by GC analysis using naphthalene as an internal standard. The values in the parentheses were the isolated yields.
[c] These experiments used a recycled catalyst; first recycle (entry 2), second recycle (entry 3), third recycle (entry 4), fourth recycle (entry 5), and fifth (entry 6). The reaction was carried out under the same as those in entry 1.

coupling reactions [19–35]. Furthermore, 4.5 g of **5a** (89% isolated yield, 99% purity by ^{1}H NMR) was obtained in a 50-mmol scale reaction (**1**; 1.1 mol%, PhCN; 30 mL, 373 K, 6 h). After the reaction was completed, the catalyst could be easily recovered by adding an excess of diethylether (the precipitation method; see Section 2). The recovered catalyst could be recycled at least five times with no significant loss of catalytic activity (entries 2–6).

3.3. Mechanistic studies

The addition of radical scavenger (2,6-di-*tert*-butyl-4-methylphenol, two equivalents with respect to **1**) and radical initiator (2,2′-azobis(isobutyronitrile), two equivalents with respect to **1**) did not change the reaction rates (profiles) or the product selectivity for the **1**-catalyzed oxidative homocoupling of **4a** under the conditions in Table 4. This suggests that free-radical intermediates (e.g., alkynyl radicals) were not involved in the present oxidative homocoupling reactions.

The reaction profile for the **1**-catalyzed oxidative homocoupling of **4a** under the conditions in Fig. 5a ([**1**], 20 mM; [**4a**], 900 mM) showed an induction period of approximately 5 min. The length of the induction period depended on the concentrations of **1** and **4a**; a decrease in the concentrations of **1** and **4a** prolonged the induction period. When the homocoupling of **4a** was carried out under the conditions in Fig. 5b ([**1**], 4 mM; [**4a**], 200 mM), the induction period was approximately 50 min. The induction period disappeared on pretreatment of **1** with **4a** under Ar atmosphere at 373 K, suggesting that the induction period was caused by the reaction of **1** with an alkyne to form the catalytically active species. Consequently, the reactivity of **1** with an alkyne (**4a**) was evaluated. To the benzonitrile solution of **1** (4 mM), 50 equivalents of **4a** with respect to **1** were added, and the solution was heated to 373 K under Ar atmosphere. Then the UV–vis spectra of the solution and the production of **5a** (by GC analysis) were monitored (Fig. 6). An induction period (approximately 50 min) was observed for the formation of **5a** (Fig. 6d) in a similar way as that for catalytic oxidative homocoupling (O_2 atmosphere) under the same conditions (Fig. 5b). During the induction period, the intensity of the absorption band at 360 nm assignable to the $N_3^- \rightarrow$ Cu(II) charge-transfer [44–46] of **1** gradually decreased, and the band almost disappeared after approximately 50 min (Figs. 6a and 6c). The IR spectrum of **1** recovered after treatment with **4a** at 373 K showed that the bands of the asymmetric and symmetric stretching vibrations of the μ-1,1-azido ligands had disappeared. These findings indicate that the azido groups were eliminated from **1** during the induction period.

In the presence of **1**, no reactions of internal alkynes, such as 2-octyne and diphenylacetylene, proceeded. Therefore, the copper species in **1** is terminally bound to an alkyne. Both the catalytic homocoupling of **4a** with Cu(I) phenylacetylide (see entry 10 in Table 3) and the stoichiometric reaction with Cu(I) pheny-

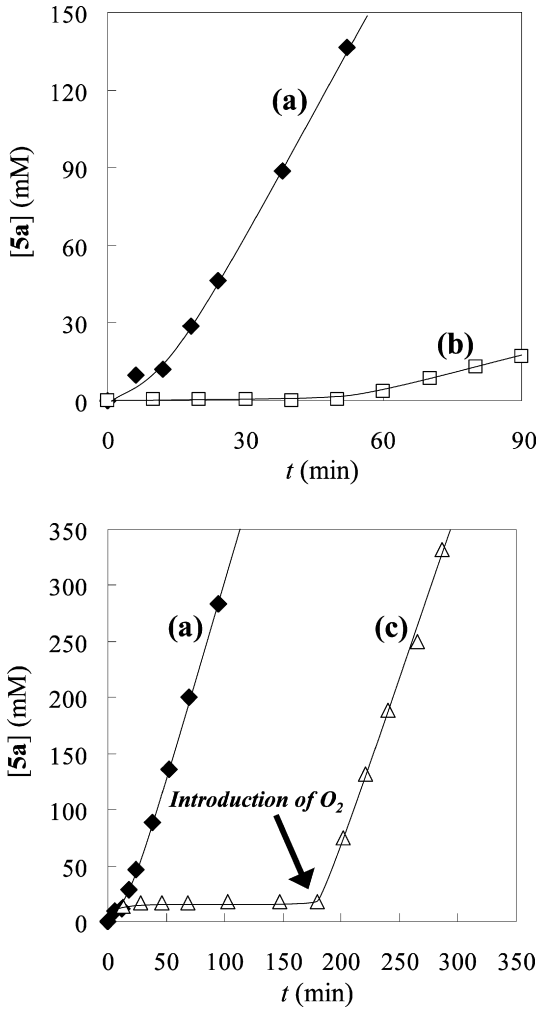

Fig. 5. Reaction profiles for the **1**-catalyzed homocoupling of **4a** under (a, b) O_2 and (c) Ar atmosphere. Reaction conditions for (a) and (c): **1** (20 mM), **4a** (900 mM), benzonitrile (1 mL), 373 K, and O_2 or Ar (1 atm). Reaction conditions for (b): **1** (4 mM), **4a** (200 mM), benzonitrile (1 mL), 373 K, and O_2 (1 atm). In the case of (c), the reaction was initially carried out under Ar atmosphere. After 180 min, 1 atm of molecular oxygen was introduced as indicated by an arrow.

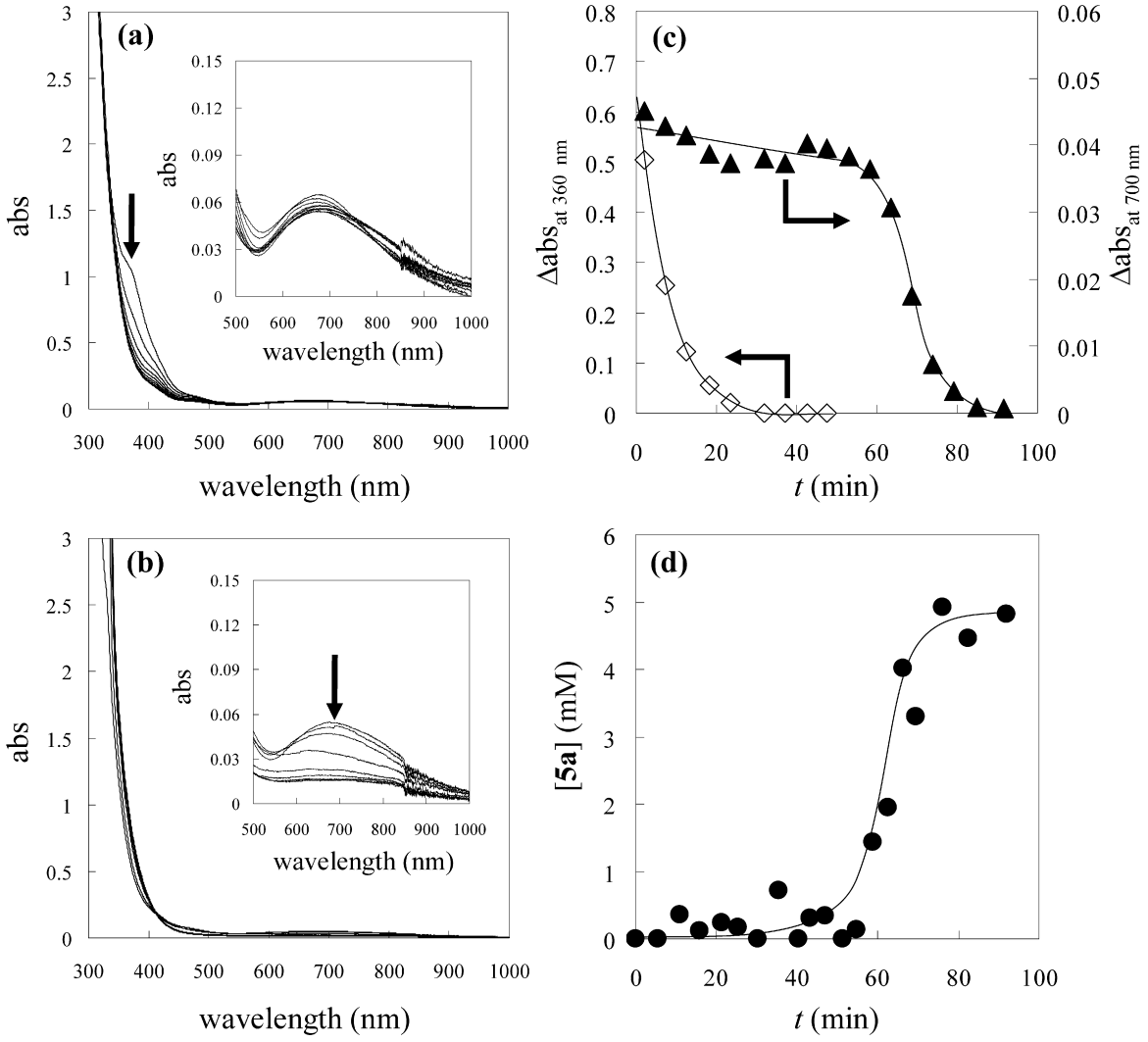

Fig. 6. Changes of UV–vis spectra ((a) ~50 min and (b) 50–100 min) for the reaction of **1** with **4a** under Ar atmosphere, and time profiles of (c) the absorbance at 360 nm and 700 nm and (d) formation of **5a**. Reaction conditions: **1** (4 mM), **4a** (200 mM), benzonitrile (1 mL), 373 K, and Ar (1 atm).

lacetylide did not proceed, suggesting that formation of Cu(I) acetylide species was not involved in the present catalytic cycle. As mentioned earlier, the di-copper core in **1** played an important role in the present oxidative alkyne–alkyne homocoupling, and it has been proposed that the copper(II)-catalyzed alkyne–alkyne homocoupling reaction proceeds via the formation of the di-copper(II)–alkynyl intermediate $\{Cu(II)_2(\mu\text{-}C{\equiv}CR)_2\}$ [16,43]. Thus, it is likely that the present homocoupling proceeded via the formation of similar di-copper(II)–alkynyl species formed by the ligand exchange between the azido groups in **1** and alkynyl groups, and that the induction period corresponded to formation of the catalytically active di-copper(II)–alkynyl species [Eq. (3)] [36]. Whereas the absorption bands of copper alkynyl species has been observed at around 370 nm [47], here the absorption band could not be detected because of the overlap with the intense absorption bands of **1**, solvent, and products.

$$2\,R{-}{\equiv} + \{Cu(II)_2(\mu\text{-}N_3)_2\} \longrightarrow \{Cu(II)_2(\mu\text{-}C{\equiv}CR)_2\} + 2N_3^- + 2H^+ \quad (3)$$

After the induction period, an almost equimolar amount of **4a** (8.8±1.0 mM) with respect to the copper(II) species in **1** (8.0 mM) was converted into **5a**, with a concomitant decrease in the absorption band at 700 nm, which can be assigned to the d–d transition of the copper(II) species in **1** (Figs. 6b–6d) [48]. These results suggest that the copper(II) species in **1** was reduced to copper(I) species [Eq. (4)] [36]. The d–d transition band of the copper(II) species again appeared when molecular oxygen was introduced to the solution, indicating that the reduced copper(I) species in **1** was reoxidized to copper(II) species by molecular oxygen [Eq. (5)] [36]. When molecular oxygen was introduced to the system after the treatment of **1** with **4a** at 373 K under Ar atmosphere, no induction period was observed, and the homocoupling of **4a** proceeded at almost the same rate as that under the catalytic turnover conditions [profile (a) vs profile (c) in Fig. 5].

$$\{Cu(II)_2(\mu\text{-}C{\equiv}CR)_2\} \longrightarrow R{-}{\equiv}{\equiv}{-}R + \{Cu(I)_2\} \quad (4)$$

$$\{Cu(I)_2\} + 2\,R{-}{\equiv} + 1/2O_2 \longrightarrow \{Cu(II)_2(\mu\text{-}C{\equiv}CR)_2\} + H_2O \quad (5)$$

Monitoring the formation of water (benzamide) for the **1**-catalyzed homocoupling of **4a** with molecular oxygen revealed that the amount of water produced was the same as that of **5a** produced, as shown in Fig. 7a. Molecular oxygen uptake during the homocoupling of **4a** also was measured. As shown in Fig. 7b, the amount of molecular oxygen consumed was half that of **5a** produced. These respective 1:1 (water formed/diyne formed) and 1:2

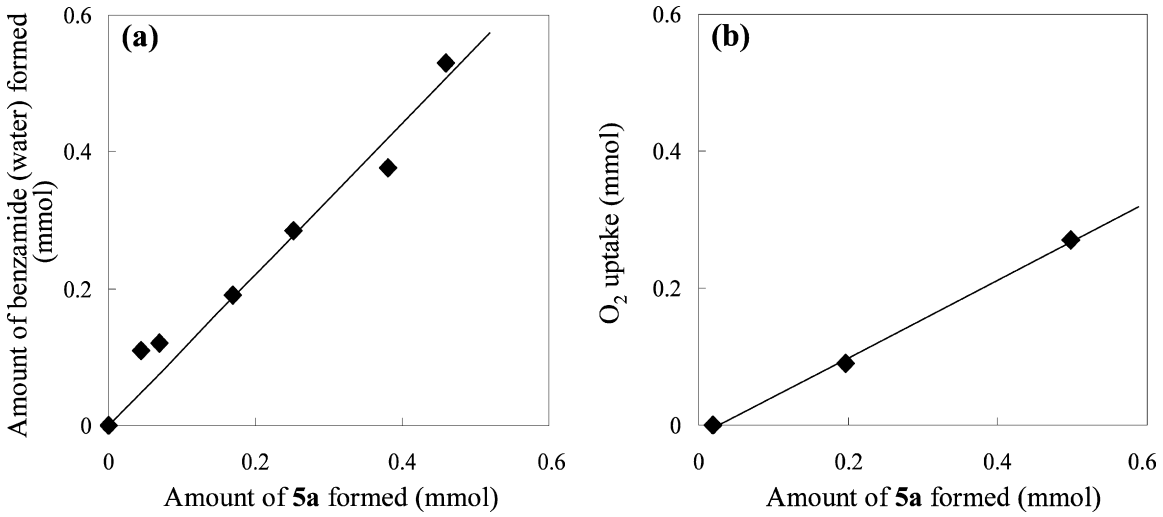

Fig. 7. (a) Relationship between amounts of **5a** and benzamide (water) formed, and (b) relationship between amounts of **5a** formed and uptake of molecular oxygen for the **1**-catalyzed homocoupling of **4a**. Reaction conditions were the same as those in Table 3. Slope of (a) (water formed/**5a** formed) = 1.11. Slope of (b) (O_2 uptake/**5a** formed) = 0.56.

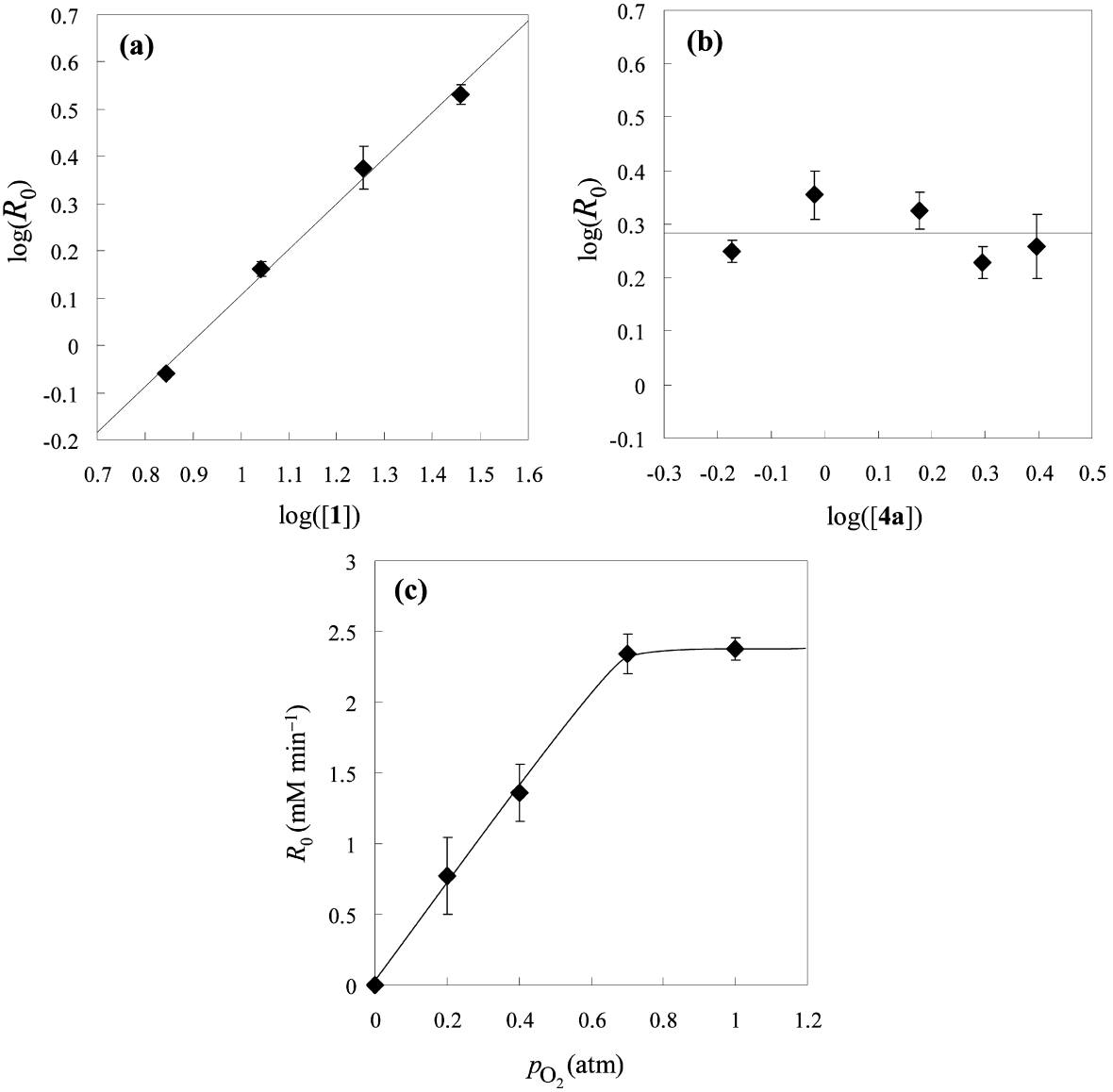

Fig. 8. Dependences of the reaction rate (R_0) on (a) the concentration of **1**, (b) the concentration of **4a**, and (c) the partial pressure of molecular oxygen for the **1**-catalyzed homocoupling of **4a**. Reaction conditions: **1** (7.0–28.7 mM), **4a** (0.7–2.0 M), benzonitrile (1 mL), 373 K, and O_2 (~1 atm).

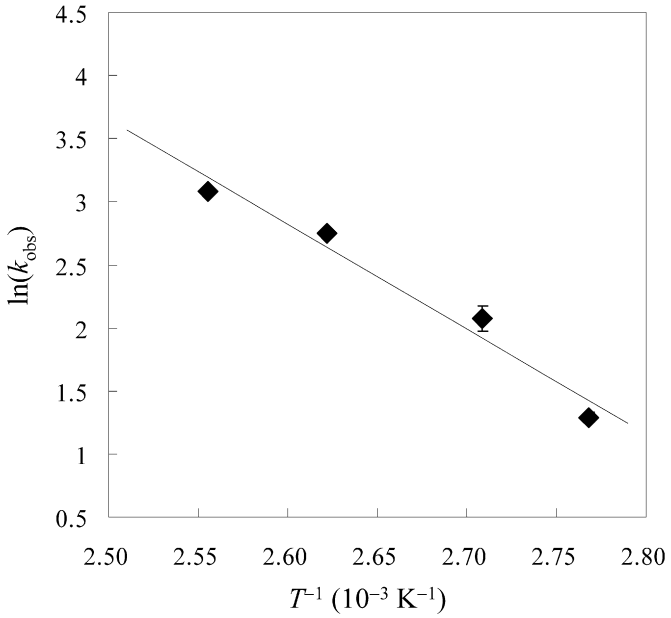

Fig. 9. Arrhenius plots for the **1**-catalyzed homocoupling of **4a**. Line fit: $\ln(k_{obs}) = 24.4 - 8296.5/T$.

(molecular oxygen consumed/diyne formed) stoichiometries support the overall reactions shown in Eqs. (4) and (5).

The initial reaction rate (R_0) for the homocoupling of **4a** showed a first-order dependence on the concentration of **1** (7.0–28.7 mM, Fig. 8) and was almost independent of both the concentration of **4a** (0.7–2.0 M, Fig. 8) and the partial pressure of molecular oxygen (>0.7 atm, Fig. 8). Good linearity of the Arrhenius plots (observed rate constant k_{obs} vs T^{-1}; Fig. 9) was seen, and the activation energy (E_a) was 68.9 kJ mol^{-1}, lower than that of the homocoupling under Hay's conditions ($E_a = 87.9$ kJ mol^{-1}) [35]. From the kinetic data, R_0 for the **1**-catalyzed homocoupling of **4a** can be expressed by the following equation:

$$R_0 = 3.93 \times 10^{10} \exp(-8.30 \times 10^3/T)[\mathbf{1}]^1[\text{alkyne}(\mathbf{4a})]^0 p_{O_2}^0. \quad (6)$$

A kinetic isotope effect was not observed for the oxidative homocoupling of ethynylbenzene (**4a**) and ethynylbenzene-d_1 (**4b**) under the conditions in Table 4 ($k_H/k_D = 1.0$), indicating that the C–H bond cleavage is not included in the rate-limiting step [49]. These results demonstrate that the formation of a diyne from di-copper(II)–alkynyl species [Eq. (4)] is the rate-limiting step.

4. Conclusion

In this work, the monomeric di-copper-substituted γ-Keggin silicotungstate with bis-μ-1,1-azido ligands **1** was synthesized, and the molecular structure was successfully determined by the X-ray crystallographic analysis. Complex **1** was present as a monomer, and no dimerization occurred in organic solvents, including acetonitrile, benzonitrile, and 1,2-dichloroethane. Complex **1** could act as an effective homogeneous catalyst for the oxidative alkyne–alkyne homocoupling. Various structurally diverse alkynes, including aromatic, aliphatic, and heteroatom-containing ones, could be converted into the corresponding diynes in high to excellent yields. The catalyst could be easily separated from the reaction mixture, and the recovered catalyst could be recycled with no significant decrease in catalytic performance. Our findings indicate that the di-copper core in **1** plays an important role and that the formation of the di-copper(II)–alkynyl species {Cu(II)$_2$(μ-C≡CR)$_2$} is the key step in the oxidative alkyne–alkyne homocoupling.

Acknowledgments

This work was supported by the Core Research for Evolutional Science and Technology (CREST) program of the Japan Science and Technology Agency (JST) and the Grants-in-Aid for Scientific Research from Ministry of Education, Culture, Sports, Science and Technology. The authors thank T. Katayama, University of Tokyo for his help with the experiments.

Supporting information

The online version of this article contains additional supplementary material.

Please visit DOI: 10.1016/j.jcat.2008.06.004.

References

[1] M.T. Pope, Heteropoly and Isopoly Oxometalates, Springer-Verlag, Berlin, 1983, pp. 1–165.
[2] C.L. Hill, C. Chrisina, M. Prosser-McCartha, Coord. Chem. Rev. 143 (1995) 407.
[3] T. Okuhara, N. Mizuno, M. Misono, Adv. Catal. 41 (1996) 113.
[4] N. Mizuno, M. Misono, Chem. Rev. 98 (1998) 199.
[5] R. Neumann, Prog. Inorg. Chem. 47 (1998) 317.
[6] I.V. Kozhevnikov, Chem. Rev. 98 (1998) 171.
[7] N. Mizuno, K. Yamaguchi, K. Kamata, Coord. Chem. Rev. 249 (2005) 1944.
[8] N. Mizuno, K. Kamata, K. Yamaguchi, in: R. Richards (Ed.), Surface and Nanomolecular Catalysis, Taylor and Francis Group, New York, 2006, pp. 463–492.
[9] A. Tézé, G. Hervé, Inorg. Synth. 27 (1990) 85.
[10] J. Ribas, A. Escuer, M. Monfort, R. Vicente, R. Cortés, L. Lezama, T. Rojo, Coord. Chem. Rev. 193–195 (1999) 1027.
[11] S. Cenini, E. Gallo, A. Caselli, F. Ragaini, S. Fantauzzi, C. Piangiolino, Coord. Chem. Rev. 250 (2006) 1234.
[12] P. Mialane, A. Dolbecq, J. Marrot, F. Sécheresse, Angew. Chem. Int. Ed. 43 (2004) 2274.
[13] P. Mialane, A. Dolbecq, J. Marrot, E. Rivière, F. Sécheresse, Chem. Eur. J. 11 (2005) 1771.
[14] P. Mialane, C. Duboc, J. Marrot, E. Rivière, A. Dolbecq, F. Sécheresse, Chem. Eur. J. 12 (2006) 1950.
[15] P. Mialane, A. Dolbecq, F. Sécheresse, Chem. Commun. (2006) 3477.
[16] P. Siemsen, R.C. Livingston, F. Diederich, Angew. Chem. Int. Ed. 39 (2000) 2632.
[17] L. Hansen, P.M. Boll, Phytochemistry 25 (1986) 285.
[18] H. Matsunaga, M. Katano, H. Yamamoto, H. Fujito, M. Mori, K. Takata, Chem. Pharm. Bull. 38 (1990) 3480.
[19] C. Glaser, Ber. Dtsch. Chem. Ges. 2 (1869) 422.
[20] A.S. Hay, J. Org. Chem. 27 (1962) 3320.
[21] I.D. Campbell, G. Eglinton, Org. Synth. 45 (1965) 39.
[22] S.M. Auer, M. Schneider, A. Baiker, J. Chem. Soc. Chem. Commun. (1995) 2057.
[23] J. Li, H. Jiang, Chem. Commun. (1999) 2369.
[24] R. Salazar, L. Fomina, S. Fomine, Polym. Bull. 47 (2001) 151.
[25] A. Sharifi, M. Mirzaei, M.R. Naimi-Jamal, J. Chem. Res. (2002) 628.
[26] J.S. Yadav, B.V.S. Reddy, K.B. Reddy, K.U. Gayathri, A.R. Prasad, Tetrahedron Lett. 44 (2003) 6493.
[27] L. Wanga, J. Yana, P. Lia, M. Wanga, C. Su, J. Chem. Res. (2005) 112.
[28] X. Lu, Y. Zhang, C. Luo, Y. Wang, Synth. Commun. 36 (2006) 2503.
[29] R. Rossi, A. Carpita, C. Bigelli, Tetrahedron Lett. 26 (1985) 523.
[30] Q. Liu, D.J. Burton, Tetrahedron Lett. 38 (1997) 4371.
[31] W.A. Herrmann, V.P.W. Böhm, C.V.K. Gstöttmayr, M. Grosche, C.-P. Reisinger, T. Weskamp, J. Organomet. Chem. 618 (2001) 616.
[32] A. Lei, M. Srivastava, X. Zhang, J. Org. Chem. 67 (2002) 1969.
[33] I.J.S. Fairlamb, P.S. Bäuerlein, L.R. Marrison, J.M. Dickinson, Chem. Commun. (2003) 632.
[34] J. Li, Y. Liang, X.-D. Zhang, Tetrahedron 61 (2005) 1903.
[35] J.-H. Li, Y. Liang, Y.-X. Xie, J. Org. Chem. 70 (2005) 4393.
[36] K. Kamata, S. Yamaguchi, M. Kotani, K. Yamaguchi, N. Mizuno, Angew. Chem. Int. Ed. 47 (2008) 2407.
[37] D.D. Perrin, W.L.F. Armarego (Eds.), Purification of Laboratory Chemicals, third ed., Pergamon Press, Oxford, 1988, pp. 80–388.
[38] L. Casella, O. Carugo, M. Gullotti, S. Garofani, P. Zanello, Inorg. Chem. 32 (1993) 2056.
[39] I.D. Brown, D. Altermatt, Acta Crystallogr. Sect. B: Struct. Sci. 41 (1985) 244.
[40] N.E. Brese, M. O'Keeffe, Acta Crystallogr. Sect. B: Struct. Sci. 47 (1991) 192.
[41] D.K. Lyon, W.K. Miller, T. Novet, P.J. Domaille, E. Evitt, D.C. Johnson, R.G. Finke, J. Am. Chem. Soc. 113 (1991) 7209.
[42] D.-L. Long, C. Streb, Y.-F. Song, S. Mitchell, L. Cronin, J. Am. Chem. Soc. 130 (2008) 1830.

[43] F. Bohlmann, H. Schönowsky, E. Inhoffen, G. Grau, Chem. Ber. 97 (1964) 794.
[44] J.E. Pate, P.K. Ross, T.J. Thamann, C.A. Reed, K.D. Karlin, T.N. Sorrell, E.I. Solomon, J. Am. Chem. Soc. 111 (1989) 5198.
[45] S. Sen, S. Mitra, D.L. Hughes, G. Rosair, C. Desplenches, Polyhedron 26 (2007) 1740.
[46] M. Allevi, M. Bonizzoni, L. Fabbrizzi, Chem. Eur. J. 13 (2007) 3787.
[47] V.W. Yam, K.K. Lo, W.K. Fung, C. Wang, Coord. Chem. Rev. 17 (1998) 17.
[48] B.J. Hathaway, D.E. Billing, Coord. Chem. Rev. 5 (1970) 143.
[49] K.A. Connors, Chemical Kinetics, The Study of Reaction Rates in Solution, VCH Publishers, New York, 1990, pp. 292–305.